IOPscience iopscience.iop.org

Home Search Collections Journals About Contact us My IOPscience

Anelasticity-induced increase of the Al-centered local symmetry in the metallic glass $La_{50}Ni_{15}Al_{35}$

This article has been downloaded from IOPscience. Please scroll down to see the full text article.

2013 J. Phys.: Condens. Matter 25 165701

(http://iopscience.iop.org/0953-8984/25/16/165701)

View the table of contents for this issue, or go to the journal homepage for more

Download details:
IP Address: 159.226.35.24
The article was downloaded on 08/04/2013 at 02:24

Please note that terms and conditions apply.

IOP Publishing Journal of Physics: Condensed Matter
J. Phys.: Condens. Matter **25** (2013) 165701 (5pp) doi:10.1088/0953-8984/25/16/165701

Anelasticity-induced increase of the Al-centered local symmetry in the metallic glass $La_{50}Ni_{15}Al_{35}$

M T Sandor[1], H B Ke[2], W H Wang[2] and Y Wu[1]

[1] Department of Physics and Astronomy, University of North Carolina, Chapel Hill, NC 27599-3255, USA
[2] Institute of Physics, Chinese Academy of Sciences, Beijing 100190, People's Republic of China

E-mail: yuewu@physics.unc.edu

Received 25 December 2012, in final form 14 February 2013
Published 3 April 2013
Online at stacks.iop.org/JPhysCM/25/165701

Abstract
The mechanism of anelastic deformation of metallic glasses is a fundamental issue of materials physics. A critical step toward atomic level understanding is the identification of measurable atomic level structural parameters that respond to anelastic deformation. We demonstrate that the electric-field-gradient tensor measured by means of ^{27}Al nuclear magnetic resonance in glassy $La_{50}Ni_{15}Al_{35}$ is such a parameter and it reveals that anelasticity induces atomic processes that lead to increases of local site symmetry at Al sites. Such atomic processes could play an important role in the reversible slow β process.

(Some figures may appear in colour only in the online journal)

Metallic glasses are a class of amorphous solids with unique structures and mechanical properties [1–5]. It is known that metallic glass structures consist of densely packed atoms, but the precise description of such amorphous structures is rather intricate [5–8]. Hence, unlike for crystalline solids where point defects and topological defects can be defined unambiguously, the structural complexity of metallic glasses makes it rather challenging to identify the key characteristics of atomic structures that are responsible for physical properties [9, 10]. On the basis of the fact that anelastic and plastic deformations of crystalline materials are related to specific atomic structures and defects such as interstitials and dislocations [11], it is not surprising that the atomic level understanding of anelastic and plastic deformations of metallic glasses is still far from complete. To achieve such fundamental understanding, it is critical to identify atomic level structural parameters that are experimentally observable and are responsive to anelastic and plastic deformations of metallic glasses. Experimental investigations of such atomic level structural parameters are extremely rare in the studies of metallic glasses [12].

Theoretical and computational studies indicate that metallic glasses deform under shear via localized shear transformations (LSTs) [13–15]. Here, a plastic core of tens and perhaps hundreds of atoms undergo non-affine transformation of cooperative shear surrounded by an Eshelby-like elastic field [4, 13, 14]. Such mesoscopic scale LSTs are thought to be the elementary steps giving rise to either plastic or anelastic deformation, depending on whether or not the surrounding elastic field is subsequently relaxed via triggering of other LSTs [4, 13, 14, 16, 17]. In contrast to the case for crystalline systems where crystal structures are directly linked to anelasticity [11], some computational studies questioned the relevance of atomistic characteristics of glass structures to the behaviors of LSTs [14, 18, 19]. Are there atomic scale characteristics that play an important role in anelastic and plastic deformations of metallic glasses?

In this work, we report ^{27}Al nuclear magnetic resonance (NMR) observation of anelasticity-induced atomic level structural changes in $La_{50}Ni_{15}Al_{35}$ bulk metallic glass (BMG). It is demonstrated that the NMR-detected electric-field-gradient (EFG) tensor at Al sites, which is a sensitive measure of the site symmetry at the Al sites [20, 21], responds to anelastic deformation of metallic glasses. The measured change of the structural parameter demonstrates that a significant fraction of Al sites undergo anelasticity-induced

 © 2013 IOP Publishing Ltd Printed in the UK & the USA

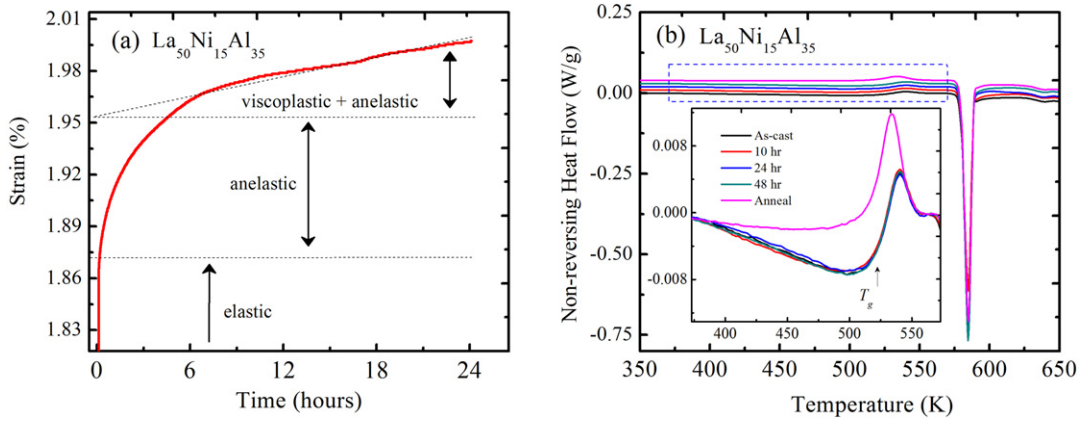

Figure 1. (a) Room temperature compression experiments carried out at 900 MPa for 24 h. The elastic (∼1.90%), anelastic (∼0.10%; delayed elastic), and anelastic and viscoplastic strain (∼0.04%) responses are noted. (b) MDSC curves of non-reversing heat flow for as-cast, annealed, and compressed samples. The compressed samples do not show changes in enthalpic recovery near T_g. This can be compared to the case of an annealed sample, that shows significant structural relaxation.

enhancement of atomic site symmetry, such as changes experienced by Al in Al-centered icosahedral clusters [5, 20, 22]. This result sheds light on the mechanisms of anelastic deformation and the slow β process, emphasizing the importance of high symmetry of Al-centered clusters in $La_{50}Ni_{15}Al_{35}$ metallic glass.

$La_{50}Ni_{15}Al_{35}$ BMG samples were prepared by arc-melting and subsequent casting in a water-cooled copper mold, forming a cylindrical sample that is 3 mm in diameter and 50 mm long. Rods ∼6 mm long were cut from the middle section of the cylinder and the ends of each rod were then carefully polished so that they were flat and normal to the cylindrical axis. Such prepared rods were then compressed under constant uniaxial stress of 900 MPa (Instron electromechanical testing system 3384), below the yield strength of 1000 MPa, for a given time duration of 10, 24, or 48 h. The amorphous nature of these samples was confirmed by means of x-ray diffraction and differential scanning calorimetry (DSC). As-cast samples and a sample annealed at $T_g - 20$ K for 48 h without the compression treatment were also studied. Figure 1(a) shows an example of a creep curve for a system at room temperature for 24 h. The strain response is characterized by three regimes: elastic (∼1.90%), anelastic (∼0.10%), and combined viscoplastic and anelastic (∼0.04%) [23, 24]. Table 1 summarizes the length of the same rod measured with a micrometer taken before the compression and at various times after the compression. The irreversible strain of ∼0.03% is in agreement with the strain curve shown in figure 1(a). Table 2 lists the irreversible strains measured with a micrometer after unloading and after more than 48 h recovery for typical samples studied in this work. The changes of enthalpy or free volume induced by deformation or annealing were examined by means of modulated DSC (MDSC) using a TA Q200 at a heating rate of 4 K min^{-1}, and temperature amplitude variation of ±2 K with a period of 60 s. Figure 1(b) shows the MDSC curves in the temperature range 350 to 650 K for the as-cast, compressed, and annealed BMG samples. The inset in figure 1(b) shows the exothermic events preceding

Table 1. Micrometer measurements for an $La_{50}Ni_{15}Al_{35}$ BMG rod before compression, immediately after compression, and 10 and 24 h after constant compression. The average irreversible strain after 24 h is ∼0.03%.

	Before	Right after	10 h after	24 h after
Length (mm)	6.4522	6.4425	6.4483	6.4501

Table 2. Fitting values of the quadrupole frequency $\omega_Q/2\pi$ and sample length changes. The Knight shift values are obtained from ^{27}Al spectra shown in figure 3. The inset in figure 3 shows that the Knight shifts of the as-cast sample and compressed samples are the same: ∼657 ppm. The decrease of the Knight shift to 647 ppm observed for the annealed sample is consistent with MDSC due to changes of the free volume.

$La_{50}Ni_{15}Al_{35}$	$\omega_Q/2\pi$ (kHz)	% irreversible length change (%)	Knight shift (ppm)
As-cast	820 ± 30	—	657
10 h	620 ± 20	0.0	657
24 h	650 ± 20	−0.03	657
48 h	530 ± 20	−0.04	657
Annealed	770 ± 30	−0.09	647

T_g that represent the excess free volume trapped in the glassy state during rapid solidification [25, 26]. Annealing causes, in comparison to the as-cast state, significant structural relaxation as evidenced by the reduction of the exothermic peak below T_g. In contrast, the compressed samples did not show any significant changes in the MDSC curves below T_g, indicating that no detectable changes of free volume and structural relaxation were induced by the compression treatment.

Atomic strain energy is one of the atomic level quantities that describes the deviation of the atomic structure surrounding a given atom i from the ideal densely packed structure [9, 10]. To the lowest order approximation and in the framework of central forces, the atomic strain energy

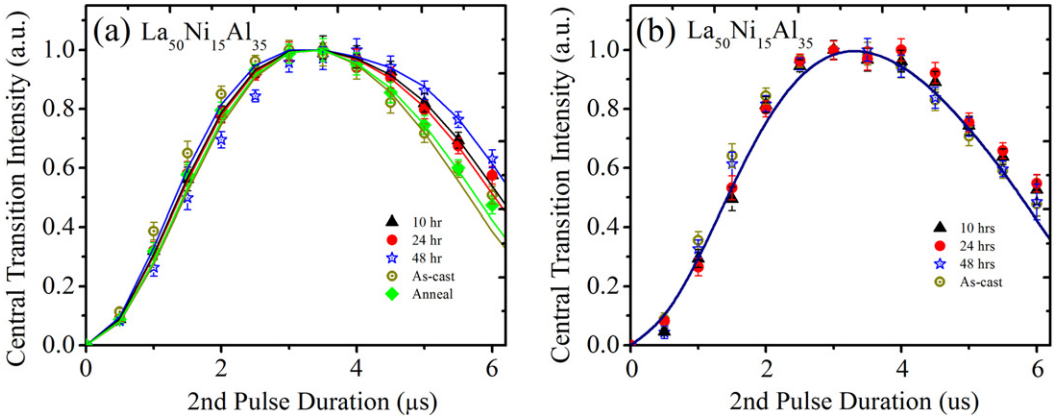

Figure 2. (a) Nutation data where the central transition intensity is plotted versus the second pulse duration in the echo sequence are shown for as-cast, annealed, and compressed samples treated at 900 MPa. Experimental errors are represented by the error bars. Solid lines are fittings of ω_Q and summarized in table 1 in addition to the percentage length changes. (b) Nutation data for as-cast, and compressed samples taken two months after the compression treatment show no significant differences in EFG. Experimental errors are represented by the error bars. The fit of the nutation curve gives $\omega_Q = 810 \pm 30$ kHz.

associated with atom i can be expressed as

$$\Delta E = (1/2)\left(\frac{\partial^2 E}{\partial \vec{r}_i^2}\right)\left(\sum_{l=0,2}\sum_{m=0,\pm l}\varepsilon_2^{l,m}(i)Y_l^m(\theta_i,\varphi_i)\right) \times |\Delta\vec{r}_i|_{\rm eq}^2|\Delta\vec{r}_i|^2 = (1/2), \quad (1)$$

where E is the internal potential energy, $\Delta\vec{r}_i$ is the displacement of atom i (the neighboring atoms are fixed) in the direction (θ_i, φ_i), $Y_l^m(\theta_i, \varphi_i)$ are the spherical harmonics, and $\varepsilon_2^{l,m}(i)$ are the atomic site symmetry coefficients. The coefficient for $l = 0$ corresponds to hydrostatic pressure and is sensitive to the local coordination number and volume whereas the $l = 2$ coefficients represent the local shear stresses that can vanish in a cubic structure as well as in any structure with higher symmetry such as icosahedral symmetry. In terms of the atomic packing surrounding atom i, $\varepsilon_2^{2,m}(i)$ describes the ellipsoidal deviation of the packing from spherical symmetry. The parameter $\beta(i) = (1/\varepsilon_2^{0,0}(i))\sqrt{\sum_{m=0,\pm2}|\varepsilon_2^{2,m}(i)|^2}$, which is invariant as regards the choice of the coordination system, is often used to represent $\varepsilon_2^{2,m}(i)$. Detection of such atomic level structural parameters has to rely on local probes, among which the NMR of quadrupolar nuclei is particularly promising.

^{27}Al NMR nutation experiments were performed in a magnetic field of 8.9 T at 300 K using an echo pulse sequence $(t_1)_x$–τ_1–$(t_2)_x$–τ_2–aquisition$_{-y}$, where t_1 and t_2 are radiofrequency (rf) pulse lengths, x and $-y$ are pulse and receiver phases, respectively, and τ_1 and τ_2 are time delays [27, 28]. The echo intensity associated with the central transition $|-1/2\rangle \leftrightarrow |1/2\rangle$ was acquired at $\tau_2 = \tau_1$. Measurements were obtained using an rf pulse strength of $\omega_{\rm rf}/2\pi = 50$ kHz and by setting $t_1 = 1$ μs and allowing t_2 to vary from 0.5 to 6.5 μs in increments of 0.5 μs. A recycle delay of 300 ms was used in signal averaging. Simulations of the nutation curves were employed to extract EFG parameters. The intensity of the central transition $|-1/2\rangle \leftrightarrow |1/2\rangle$ is determined by the evolution of the density operator $\rho(t_1, \tau_1, t_2, \tau_2)$ governed by the Hamiltonian $H = \omega_{\rm rf}I_z + H_Q^{(1)}$ during the periods of t_1 and t_2 and by $H_Q^{(1)}$ during the periods of τ_1 and τ_2. Here, the Hamiltonian $H_Q^{(1)}$ is the first-order quadrupole interaction given by $H_Q^{(1)} = C_Q V_{20} T_{20}$, where $C_Q = eQ/[2I(2I-1)\hbar]$, Q is the electric quadrupole moment and $I = 5/2$ for ^{27}Al nuclei, $T_{20} = (1/\sqrt{6})[3I_z^2 - I(I+1)]$ and I_z is the nuclear spin operator along the external magnetic field, and V_{20} is a component of the second-rank irreducible EFG tensor V_{2m} in the laboratory frame (x, y, z) where the z-axis is along the external magnetic field [28]. In the principal axis system (PAS) (X, Y, Z) of the EFG tensor, the diagonal components are V_{ZZ}, V_{YY}, V_{XX} ($|V_{ZZ}| \geq |V_{YY}| \geq |V_{XX}|$), and V_{20} can be expressed as [28]

$$V_{20} = V_{ZZ}\sqrt{\frac{4\pi}{5}}\left(\sqrt{\frac{3}{2}}Y_2^0(\theta,\phi) + \frac{1}{2}\eta Y_2^2(\theta,\phi) + \frac{1}{2}\eta Y_2^{-2}(\theta,\phi)\right), \quad (2)$$

where $\eta = (V_{XX} - V_{YY})/V_{ZZ}$ and (θ, ϕ) are the polar angles of the external magnetic field in the PAS system. Often, the quadrupole frequency $\omega_Q = 3C_Q V_{ZZ}$ is used to describe the quadrupole interaction. The EFG tensor vanishes under cubic and higher symmetries such as icosahedral symmetry. By comparing equations (1) and (2) it is clear that the quadrupole interaction $H_Q^{(1)} = C_Q V_{20} T_{20}$ and the atomic strain energy carry similar structural information as regards the structural symmetry around Al, with the former represented by ω_Q and the latter by β(Al).

Figure 2(a) shows ^{27}Al NMR nutation curves of the central transition intensity versus the second pulse length t_2 for as-cast, annealed, and compressed $La_{50}Ni_{15}Al_{35}$ BMG samples several days after the compression treatment. No obvious changes of the nutation curves were noticeable within the first ten days after the compression. Simulations of the nutation curves [27] are shown as solid lines in figure 2(a) where η is fixed at 0.9 and the extracted values and associated

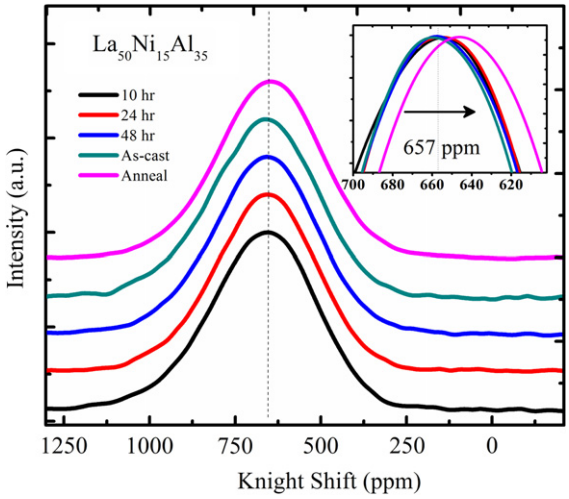

Figure 3. Spectra for the as-cast, compressed, and annealed rods are shown. The inset demonstrates the small change in Knight shift from 657 to 647 ppm caused by structural relaxation.

errors of $\omega_Q/2\pi$ are listed in table 2. Compression treatment under 900 MPa results in a decrease of $\omega_Q/2\pi$, and the longest compression time of 48 h gives rise to the largest decrease from 820 kHz in the as-cast sample to 530 $\pm$ 20 kHz after compression. Within the extracted errors of the simulated nutation curve, these results demonstrate that compression treatment leads to a reduced $\omega_Q/2\pi$, which implies higher local symmetry at the Al sites. Furthermore, longer compression time leads to larger decrease of $\omega_Q/2\pi$. The $\omega_Q/2\pi$ value of the annealed sample is 770 $\pm$ 30 kHz. This shows that although the local site symmetry might be slightly increased upon annealing, it is comparable to that of the as-cast sample within simulated errors. This result and the MDSC data shown earlier demonstrate that the observed decrease of $\omega_Q/2\pi$ after compression is not due to structural relaxation but due to local structural changes induced by shear. Figure 2(b) shows nutation curves for compressed samples measured two months after the compression treatment along with the as-cast data. The data show that the $\omega_Q/2\pi$ values of the as-cast sample and the compressed samples are all the same (810 kHz) within experimental errors. This demonstrates that the decrease of $\omega_Q/2\pi$ observed soon after compression is caused by anelastic structural changes. All these NMR experiments with compressed samples have been repeated several times using various batches of BMG samples.

Although structural relaxation by annealing has minor effect on the EFG tensor, the increased density could change the electronic density of states. Figure 3 and the inset show spectra of the as-cast, annealed, and compressed samples. The spectral shift is dominated by the Knight shift $K = K_s + K_d$ [29]. K_s is the direct Fermi contact interaction represented by $K_s = (8\pi/3)|\psi(0)^2|\Omega\chi_s$, where $|\psi(0)^2|$ is the probability density of conduction electrons at the nucleus averaged over the Fermi surface and normalized by the atomic volume Ω, and χ_s is the Pauli paramagnetic volume susceptibility of s electrons. K_d is the core-polarization shift from indirect s–d

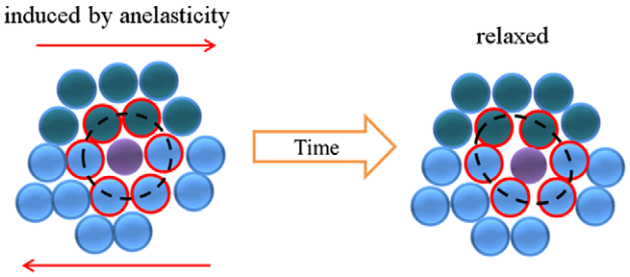

Figure 4. Illustration: an Al-centered cluster with higher symmetry relaxes back to the original state of lower symmetry under the influence of the back stress of the surrounding elastic matrix.

exchange interaction given by $K_d = \alpha_d\chi_d$, where α_d is the hyperfine coupling constant and χ_d is the Pauli susceptibility due to La and Ni d electrons. The inset in figure 3 shows that the Knight shifts (listed in table 2) of the as-cast sample and compressed samples all take the same value: ~657 ppm, whereas a notable decrease of the Knight shift to 647 ppm is observed for the annealed sample. The change in the Knight shift is predominantly due to changes of the d electron density of states [30, 31]. K_d is determined by the Al 3s valence charge transfer to the 5d band of Ni or La [32]. These results show that the different coefficients ($l = 0, 2$) of the atomic strain energy can be probed by NMR—such as the Knight shift which is sensitive for detecting the change of the scalar quantity related to the free volume and the EFG which is sensitive for detecting the change of the site symmetry induced by shear.

The slow relaxation time of local structure at room temperature, on the order of a month, shows that the process is an activated one with relaxation time $\tau = \tau_0 \exp(H_{act}/k_BT)$. Since the temperature dependence of the relaxation time is not measured, we assume $\tau_0 = 10^{-13}$ s on the basis of the typical vibrational attempt frequency. For $\tau = 2.6 \times 10^6$ s at room temperature, this gives rise to $H_{act} = 1.2$ eV. For $\tau_0 = 10^{-20}$ s [33] the corresponding estimated activation enthalpy is $H_{act} = 1.5$ eV. Such activation enthalpy is comparable to the activation energy of the slow β process suggested for analogous metallic glass systems [34]. An empirical relationship between the activation energy E_β of the β process and T_g was found to be $E_\beta = 26 \times RT_g$, where R is the gas constant [34]. With $T_g = 523$ K, $E_\beta = 1.2$ eV, which is in agreement with the estimated activation enthalpy of 1.2 eV. This is also consistent with the view of the slow β process being a local reversible event moving within the megabasin of the potential energy landscape [17]. The anelasticity-induced local structural change could involve subtle collective rearrangement of atoms around Al. As illustrated in figure 4, the rearrangement leads to subtle symmetry increase of the Al-centered clusters such as a distorted icosahedral cluster becoming a more ideal icosahedral cluster. The fact that NMR can be used to detect changes of symmetry indicates that nearly all Al sites experience improved symmetry. The average EFG detected by means of NMR would not show clear changes if only a small fraction (such as 20%) of Al sites experience improved site symmetry or in the situation where some Al sites

experience increased while other sites experience decreased site symmetry. It is interesting to note that atomic clusters were suggested to be the basic building blocks of metallic glass structures [6–8, 22, 35]. This is consistent with the current observation of the importance of Al-centered clusters in the anelastic deformation process of $La_{50}Ni_{15}Al_{35}$ bulk metallic glass.

In summary, ^{27}Al nutation NMR shows that anelasticity of $La_{50}Ni_{15}Al_{35}$ bulk metallic glass induces increased local site symmetry at the majority of Al sites. The estimated activation enthalpy associated with this reversible atomic rearrangement is consistent with the estimated activation energy of the slow β relaxation process. The results demonstrate the importance of Al-centered clusters in the anelastic deformation process and suggest that Al-centered clusters are important structural units that determine the properties of the metallic glass $La_{50}Ni_{15}Al_{35}$.

Acknowledgments

This work was supported by the US Army Research Office under Contract No. W911NF-09-1-0343 (MTS and YW) and NSF of China under Contract No. 50921091 (HBK and WHW).

References

[1] Johnson W L 1999 *MRS Bull.* **24** 42
[2] Inoue A 2000 *Acta Mater.* **48** 279
[3] Wang W H, Dong C and Shek C H 2004 *Mater. Sci. Eng.* R **44** 45
[4] Schuh C A, Hufnagel T C and Ramamurty U 2007 *Acta Mater.* **55** 4067
[5] Cheng Y Q and Ma E 2011 *Prog. Mater. Sci.* **56** 379
[6] Sheng H W, Luo W K, Alamgir F M, Bai J M and Ma E 2006 *Nature* **439** 419
[7] Hwang J, Melgarejo Z H, Kalay Y E, Kalay I, Kramer M J, Stone D S and Voyles P M 2012 *Phys. Rev. Lett.* **108** 195505
[8] Miracle D B 2004 *Nature Mater.* **3** 697
[9] Egami T 2011 *Prog. Mater. Sci.* **56** 637
[10] Egami T, Maeda K and Vitek V 1980 *Phil. Mag.* A **41** 883
[11] Nowick A S and Berry B S 1972 *Anelastic Relaxation in Crystalline Solids* (New York: Academic)
[12] Dmowski W, Iwashita T, Chuang C P, Almer J and Egami T 2010 *Phys. Rev. Lett.* **105** 205502
[13] Argon A S 1979 *Acta Metall.* **27** 47
[14] Rodney D, Tanguy A and Vandembroucq D 2011 *Modelling Simul. Mater. Sci. Eng.* **19** 083001
[15] Falk M L and Langer J S 2011 *Annu. Rev. Condens. Matter Phys.* **2** 353
[16] Johnson W L and Samwer K 2005 *Phys. Rev. Lett.* **95** 195501
[17] Harmon J S, Demetriou M D, Johnson W L and Samwer K 2007 *Phys. Rev. Lett.* **99** 135502
[18] Maloney C E and Lemaître A 2006 *Phys. Rev.* E **74** 016118
[19] Dasgupta R, Karmakar S and Procaccia I 2012 *Phys. Rev. Lett.* **108** 075701
[20] Xi X K, Li L L, Zhang B, Wang W H and Wu Y 2007 *Phys. Rev. Lett.* **99** 095501
[21] Xi X K, Sandor M T, Liu Y H, Wang W H and Wu Y 2009 *Scr. Mater.* **61** 967
[22] Cheng Y Q, Ma E and Sheng H W 2009 *Phys. Rev. Lett.* **102** 245501
[23] Taub A I and Spaepen F 1981 *J. Mater. Sci.* **16** 3087
[24] Lee S C, Lee C M, Lee J C, Kim H J, Shibutani Y, Fleury E and Falk M L 2008 *Appl. Phys. Lett.* **92** 151906
[25] van den Beukel A and Sietsma J 1990 *Acta Metall. Mater.* **38** 383
[26] Slipenyuk A and Eckert J 2004 *Scr. Mater.* **50** 39
[27] Man P P 1993 *Solid State Nucl. Magn. Reson.* **2** 165
[28] Freude D and Haase J 1993 *NMR Basic Princ. Prog.* **29** 1
[29] Carter G C, Bennett L H and Kahan D J 1977 *Prog. Mater. Sci.* **20** 1
[30] Yang D P, Hines W A, Tsai C L, Giessen B C and Lu F C 1991 *J. Appl. Phys.* **69** 6225
[31] Yamamoto I, Van Zytveld J and Endo H 1993 *J. Non-Cryst. Solids* **156/158** 302
[32] Yang D P 1988 *PhD Thesis* The University of Connecticut
[33] Hennig J, Mari D and Schaller R 2009 *Phys. Rev.* B **79** 144116
[34] Yu H B, Wang W H, Bai H Y, Wu Y and Chen M W 2010 *Phys. Rev.* B **81** 220201
[35] Ma D, Stoica A D, Wang X L, Lu Z P, Clausen B and Brown D W 2012 *Phys. Rev. Lett.* **108** 085501